TRANSPORT
ISSN 1648-4142 / eISSN 1648-3480
2019 Volume 34 Issue 1: 41–51
https://doi.org/10.3846/transport.2019.7081

PEDESTRIAN SAFETY: A NEW METHOD TO ASSESS PEDESTRIAN KINEMATICS

Mariusz PTAK*

Faculty of Mechanical Engineering, Wroclaw University of Science and Technology, Poland

Received 16 February 2018; revised 19 April 2018; accepted 15 May 2018

Abstract. The progress in pedestrian safety enhancement is the result of multi-stage work, which is based mainly on the vehicle enhancement and appropriate traffic organization. However, the full separation of vehicle traffic and pedestrians seem to be impossible nowadays. The paper presents a new method for assessing the influence of vehicle structural components on pedestrian kinematics. An integral part of the method is the relationship, named as the *k* parameter, which can determinate the geometric property of the pedestrian body movement (kinematics) after a collision. The development of the new algorithm is the answer to the problem of assessing the risk posed by the impact of the vehicle with a high bumper/bonnet reference line (e.g. a Sport Utility Vehicle – SUV) on a pedestrian. The presented method can be a useful engineering tool to assess the safety of vehicles, both brand-new and used. The developed test system binds together a new defined kinematic criterion as well as the existing biomechanical criteria (the assessment of vehicles using pedestrian impactors). The presented method was verified on a compact vehicle and a SUV.

Keywords: pedestrian, numerical simulation, vehicle design, traffic accident, traffic safety, kinematics, MADYMO.

Introduction

The Vulnerable Road User (VRU) safety is an important consensus between many critical factors such as vehicle design, its frontal aggressiveness, roads and pavements layout, legislations, active and passive safety systems or bicyclist's helmet. Pedestrians form the second largest group of road fatalities as around than one-third of seriously injured or killed people account for VRUs in EU (EC 2015; Ptak *et al.* 2012; Simms *et al.* 2015). Motorcyclist's share of all road deaths adds, on average in EU, 15% to this statistics (EC 2015). The disproportion in pedestrian injuries and fatalities strongly correlates with roads and pavements infrastructure, speed limits and the national health care systems (Asaithambi *et al.* 2016; Kadali, Vedagiri 2016; Nordfjærn, Zavareh 2016). Additionally, the examination of the mobility trends in the EU countries shows growth of walking usage as a mean of transport. The fact that more people choose to walk or use a bike is essentially a good development for the EU and in line with the need for greener transport. The collated the data reported for 25 EU members of killed pedestrians correlates strongly with countries' proper infrastructure, which encourage inhabitants to choose a walking or cycling as a safe mean of transport (Levulytė *et al.* 2016, 2017). The high share of pedestrian fatalities features relatively new EU Member States as in Romania, Latvia, Poland and Lithuania where pedestrians contribute to more than 30% of all road deaths (EC 2015; Levulytė *et al.* 2017; Sokolovskij, Prentkovskis 2013).

Despite many years of research and experiments conducted by various organizations and research and industrial centers, there is still no accurate method, that would also be quick and convenient, of assessing the influence of the vehicle's front-end on the safety of VRUs. No methods have been proposed for assessing the influence of structural components of a motor vehicle on pedestrian safety, by analysing the kinematic parameters of the struck pedestrian. The current type-approval tests, based on tests with impactors, do not include the full kinematics of vehicle impact with a pedestrian, which are very significant in terms of injuries sustained by the pedestrian. The literature does not offer a criterion for determining the geometric properties of pedestrian motion after a collision with a motor vehicle. Thus, this paper examines many aspects relating to the safety of pedestrians, with main focus on vehicle front-end geometry. Finally, the author develop the test system, which binds together a new defined kinematic criteria with the existing biomechanical criteria.

E-mail: *mariusz.ptak@pwr.edu.pl*

1. State of the art

The impact of a vehicle with a VRU has already been thoroughly studied and described in several publications, mainly through tests on human cadavers (Anderson *et al.* 2007; Cesari *et al.* 1985; Kerrigan *et al.* 2012), validation against real-life accident data and increasingly popular testing on pedestrian dummies, carried out mainly in Japanese centers (Matsui *et al.* 2005; Yasuki, Yamamae 2010). The pedestrian and cyclist side impact test is the most commonly performed test since, according to Jarrett, Saul (1998) and Yang (2005), it accounts for approximately 80% of VRU accidents, who are most often hit while crossing the road (Jurecki, Stańczyk 2014).

The critical factor for VRU passive safety is the car design and its frontal aggressiveness. The existing safety research has focused on the front-end of passenger vehicle, since they contribute to majority of the accidents involving pedestrians. Many significant advances have been made in vehicle fronts (Kaczyński, Bartczak 2014; Ptak, Karliński 2012). Cars have become more streamlined and their front bumpers lost the sharp edges that could potentially increase injuries sustained by VRU in a collision. On the other hand, the recent lifestyle trend toward so-called Sport Utility Vehicles (SUV). The SUV was defined by the IMPROVER (2006) consortium.

Nevertheless, on the roads of the EU countries, vehicles with steel or alloy bumpers are rare as these gave way to plastic bumpers. Moreover, pedestrian safety issues triggered legislation changes that made car manufacturers remove corporate symbols from the front of the vehicles. The car models produced today no longer have rigid characteristic stars, leaping jaguars or recognizable ornaments, such as the Spirit of Ecstasy, which decorates the grille of Rolls-Royce vehicles. If any such element remains, it must not endanger the VRU. However, the reduction of the number of hard spots in joints and seams is still a goal of engineers (Chybowski *et al.* 2014; Zalewski, Szmidt 2014; Żółkiewski 2011), where the popping-up bonnet and pedestrian airbag contribution is significant. Additionally, the development of crash safety standards, which initially improved the vehicle occupants' passive safety, turned the global attention to vehicle safety issues. All of the above aspects are the safety countermeasures, which help to reduce VRU injuries during an impact (Fernandes *et al.* 2014). Thus, there are called passive safety elements. In other words, the passive solutions encompass design modifications to the vehicle in order to minimize the risk of injury to pedestrians and cyclist, but they do not influence vehicles handling, driver's actions or enforce autonomous manoeuvres.

The stated passive safety technologies have enabled great progresses in death and injury prevention. The influence of the vehicle's front-end on the injuries sustained by the pedestrian was described by Simms and Wood (2009). They noted that the kinematics of a pedestrian struck by a compact vehicle is significantly different from the body movement of a pedestrian hit by a vehicle with a high bumper and bonnet reference line. The difference is mainly due to the height of the contact area between the vehicle and the pedestrian's body. In the case of a SUV, the point of impact is closer to the pedestrian's center of mass than in the case of a collision with a compact vehicle.

The categorization of vehicles according to their front-end geometry, was the basis for research, which showed that a pedestrian struck by a SUV is twice as likely to die as a pedestrian hit by a compact vehicle (Lefler, Gabler 2004). Based on data from 552 cases Roudsari *et al.* (2004) estimated that the risk of a pedestrian dying in a collision with a SUV or commercial vehicle increases more than 3 times compared with a passenger vehicle. This view is also shared by Henary *et al.* (2003), although he additionally underlines that the difference in pedestrian injuries resulting from the vehicle front-end geometry, is greatest at impact speeds below 30 km/h. This is an important observation since most accidents involving pedestrians occur at speeds up to 50 km/h (Otte 1999). Above this speed the probability of survival drops dramatically (Anderson *et al.* 1997; Jurecki, Stańczyk 2014; Rosén *et al.* 2011). Based on multibody simulations and collisions with Polar II mannequins, Hamacher *et al.* (2012) concluded that the SUV is the most dangerous type of vehicles (compared to compact cars, sedans, vans, sports cars and mono-box vehicles) with respect to post-impact pedestrian kinematics. Nonetheless, numerous publications show that regardless of the type of vehicle, an increase in impact speed is directly associated with the severity of injuries sustained by the pedestrian (Lefler, Gabler 2004; Simms, Wood 2006, 2009; Zhang *et al.* 2008).

In regard with car-to-pedestrian frontal impacts, 80% of the accidents may be classified into one of the typical scenarios. The remaining 20% includes the pedestrian dragging circumstance, which is also depicted in Figure 1 where the authors numerically simulated the phases of accidents basing on Ptak *et al.* (2012) and Teresiński (2005). The mechanism of the impact was determined for the 50-percentile MADYMO male dummy in the standing stance and struck from the side by a front of vehicle – this is a typical situation encompassing 80% car-to-pedestrian collisions (Kolla *et al.* 2014; Ptak *et al.* 2017b). Pedestrian kinematics after vehicle impact was depicted in Figure 1.

It should be noted that the configuration depends primarily on the bumper and bonnet reference line relative to the pedestrian center of mass. Thus, for a 5-percentile woman the forward projection may occur during a collision with a standard compact vehicle. Conversely, the same scenario involving a 95-percentile male pedestrian will likely result in wrap projection due to the higher pedestrian center of mass. In view of the above, a collision with a small child and compact vehicle can be characterized by a similar configuration as the kinematic of a tall pedestrian (>1.74 m) stuck by a high bonnet vehicle such as SUV.

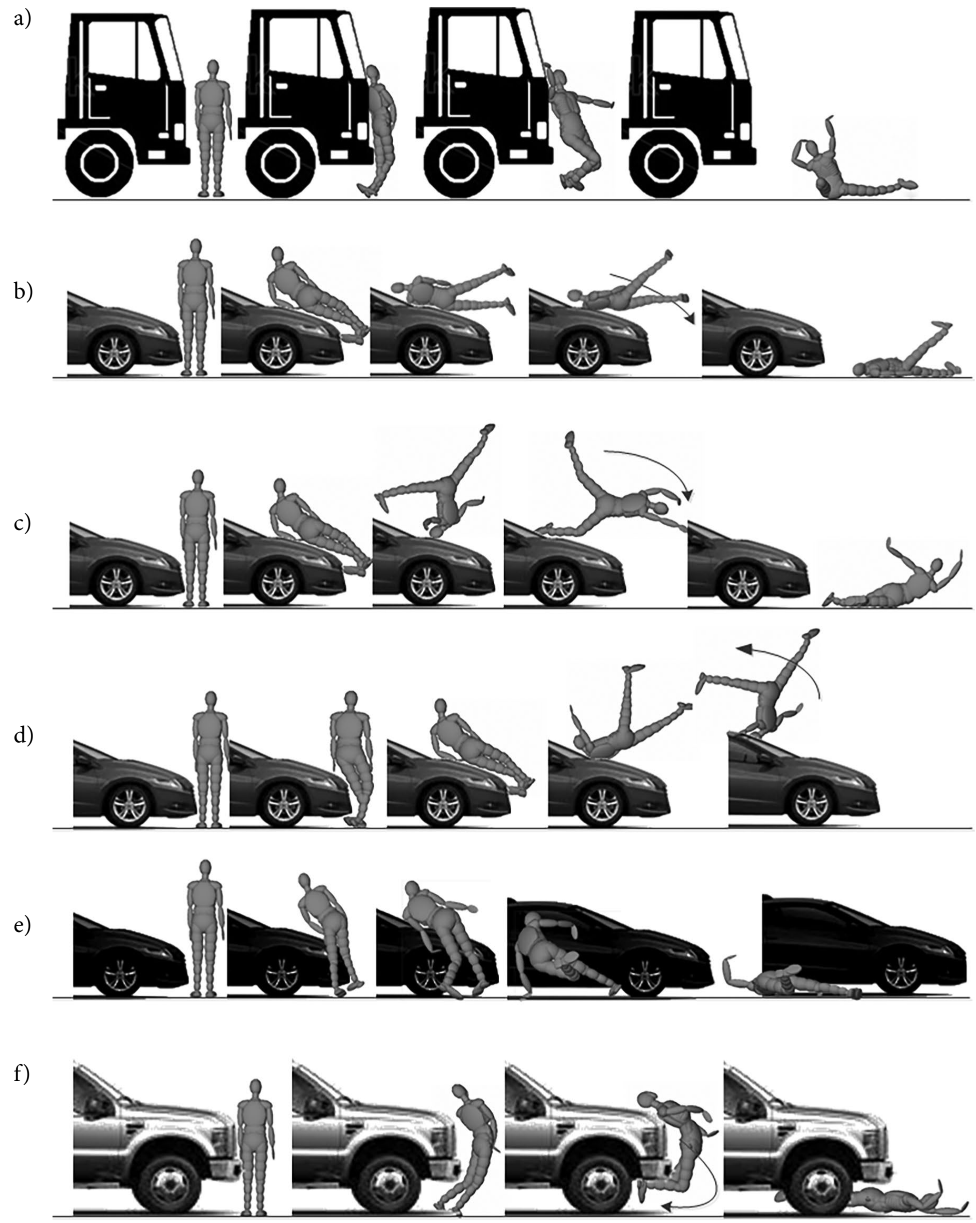

Figure 1. Pedestrian kinematics after various vehicle impacts: a – forward projection; b – wrap; c – somersault; d – roof vault; e – fender vault; f – dragging

2. Methodology

The impact configurations were necessary to understand the causes of injuries to pedestrians and to develop a method of assessing the kinematics of the pedestrian. Type-approval tests using impactors do not include the full kinematics of vehicle impact with a pedestrian, which are very significant in terms of injuries sustained by the pedestrian. The results numerical tests show significant differences in the knee joint bending for the dummy and the impactor (Kopczyński *et al.* 2011; Matsui 2004; Ptak *et al.* 2012). These discrepancies are rooted in three main parameters that distinguish the dummy from the legform impactor, namely:

- the position of the center of gravity – if the pedestrian is struck by a vehicle with a high bonnet line, the motion kinematics of the impactor is significantly changed by the following:
- the height of the center of mass above the ground: around 530 mm for the impactor and 970 mm for the 50-percentile male dummy, which served as the basis for the impactor design;
- the lack of representation of the upper body in the case of an impactor;
- the friction in the dummy acts between the foot and the ground, whereas in the case of the impactor striking the front of the vehicle, the interaction between the ground and the base of the impactor does not occur due to free flight.

The kinematic criterion has been developed in order to validate the kinematics of the pedestrian after a collision with a motor vehicle. As mentioned earlier, a mere evaluation of the biomechanical criterion, described in *Regulation (EC) No 78/2009* (EC 2009b), does not allow one to determine whether, after being struck by the vehicle, the pedestrian: is *dragged/forward projected or wrap over the bonnet.* If the kinematic criterion is satisfied, it ensures the proper impact configuration for the pedestrian – i.e. the pedestrian is wrapped over the bonnet. Failure to meet the criterion would indicate that the pedestrian is bounced off the vehicle or dragged underneath it.

The study on the kinematic criterion was a multi-stage research project and included three major components: the dummy, the vehicle and the parameters of pedestrian kinematics.

2.1. Pedestrian dummy model

It was decided to use an ellipsoidal pedestrian dummy from the MADYMO v7.5 library. This dummy is widely used in pedestrian safety tests and its biofidelity has been confirmed by numerous independent institutions (Crocetta *et al.* 2015; Ptak, Konarzewski 2015; Ratajczak *et al.* 2016; Simms *et al.* 2015). In addition, the Finite Element Method (FEM) dummy (e.g. the THUMS v4 model (DYNAmore 2018)) introduces a number of parameters which are not essential for the correct representation of kinematics, and can introduce many complications into the calculations (Ishikawa *et al.* 1993; Pezowicz, Głowacki 2012). MADYMO dummies also do not require large computing power, which, in view of the predicted number of impact configurations (80) was undoubtedly an advantage. Two dummies were used in tests: the 50-percentile male and 5-percentile female, both in their basic stance. Anthropometric data of dummies are shown in Table.

Based on the results of tests (Fricke 1990; Stevenson 2006), the contact point between the dummy and the ground was defined as well as the appropriate coefficient of friction between the soles of the dummy's shoes and the ground (asphalt), equal to 0.55. The dummy was positioned in such a way that, at the point of contact with the vehicle model described below, the dummy's legs were loaded with the mass of the dummy, and its shoes were in contact with the ground. During the entire simulation, the dummy was in the field of acceleration $g = 9.81$ m/s^2.

2.2. Vehicle model – representation of essential structural elements

Modelling of the vehicle was essential in the development of the kinematic criterion. The design requirement for the front end of the vehicle was to build an uncomplicated and parametric model. The model was to be constructed in such a way that its geometric characteristics were measurable using basic measuring tools, such as measuring ruler and protractor. In other words, these measurement tools could be used to identify key dimensions of the actual vehicle, in a non-invasive manner.

After analysing the work of Mizuno (2003, 2005) relating to testing of vehicles in terms of pedestrian safety, it was decided to define two parameters that define the vehicle's front-end geometry. The choice of the parameters listed below was influenced by the fact that both parameters are precisely defined in *Commission Regulation (EC) No 631/2009* (EC 2009a). The chosen parameters that define the front-end geometry of the vehicle are the Lower Bumper Reference Line (LBRL) and the Bonnet Leading Edge (BLE). These are illustrated and defined in Figure 2.

The points defined by LBRL and BLE serve as the centers of symmetry of ellipsoids with semi-axes $R = 70$ mm. The dimensions of both ellipsoids were determined on the basis of the outlines of vehicles described in the work of Mizuno (2003, 2005) and author's own studies on vehicles (Ptak *et al.* 2012).

Both ellipsoids form a rigid body system, which moves with an initial velocity of 40 km/h in the *Y*-axis (Figure 3). The initial velocity of the ellipsoid corresponds to the impact velocity of the legform impactor into the vehicle, according to the *Regulation (EC) No 78/2009* (EC 2009b). The total mass of the ellipsoids is 1100 kg and is many times greater than the mass of the pedestrian dummy. The delay of the ellipsoid system was not defined deliberately due to the differences in the stopping distances of vehicles.

Table. Anthropometric data of ellipsoidal dummies (TNO 2012)

Parameters / Type	Height of standing dummy [m]	Height of seated dummy [m]	Shoulder width [m]	Knee height [m]	Dummy mass [kg]	The height of the center of mass [m]
50-percentile male 	1.74	0.92	0.47	0.54	75.7	0.97
5-percentile female 	1.53	0.81	0.40	0.47	49.8	0.86

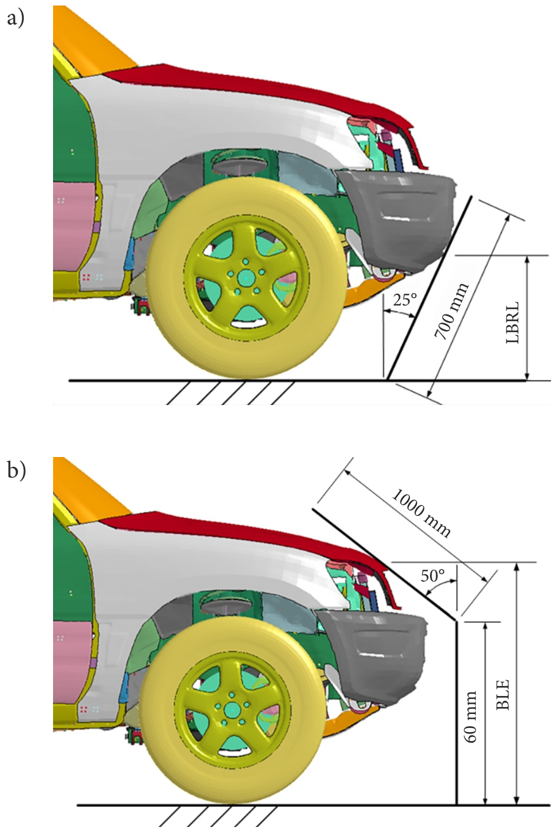

Figure 2. Chosen parameters that define the front-end geometry of the vehicle: a – Lower Bumper Reference Line (LBRL); b – Bonnet Leading Edge (BLE)

In addition, while braking, the front of the vehicle dips downward thereby lowering the height of the LBRL and BLE. Consequently, the delay and the related change in the height of the vehicle's front-end are additional parameters that were not essential in the development of the kinematic criterion. The MADYMO software was used to determine the characteristics of the force of contact between the ellipsoids. The dummy is positioned sideways in relation to the impact, in accordance with statistical data by Jarrett, Saul (1998) and Yang (2005).

The parameters of the vehicle model were as follows (Figure 3):

- *LBRL:* ranging from 70 to 970 mm, at 100 mm intervals;
- *BLE:* ranging from 520 to 1420 mm, at 100 mm intervals;
- *D:* the longitudinal distance between the axes of the ellipsoids ranging from 0 to 300 mm at 100 mm intervals.

Thus, the configuration of parameters covered most typical vehicles ranging from sports cars with a wedge-shaped body, to SUVs, to cars with a cab over engine. Please note that the author's understanding of a typical vehicle is one whose parameter $D \geq 0$ mm. Figure 4 shows typical vehicles in two categories with the marked system of ellipsoids that define LBRL and BLE.

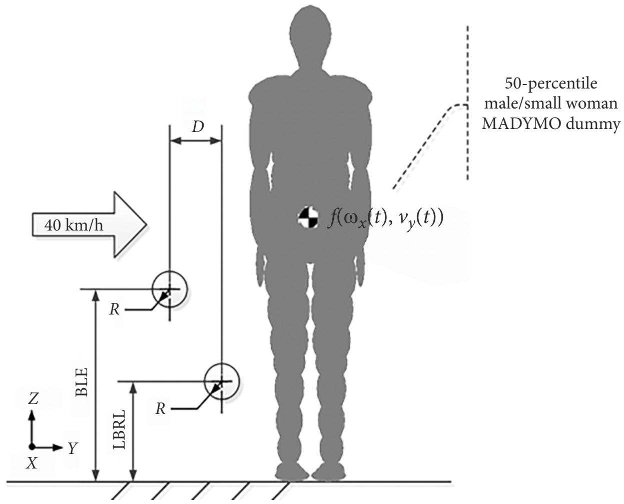

Figure 3. Determination of parameters for the vehicle's front-end model in comparison with a pedestrian dummy

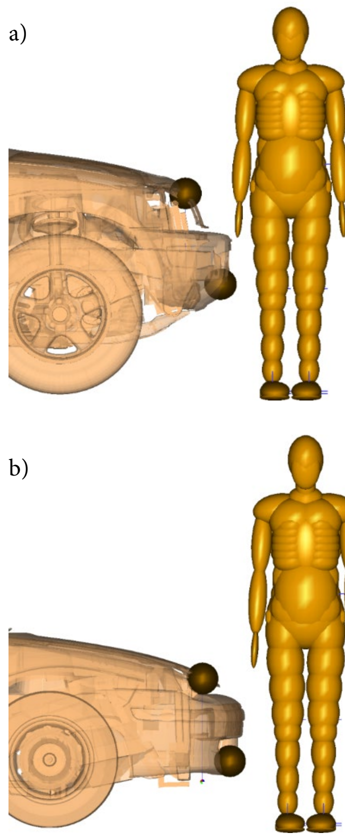

Figure 4. The system of ellipsoids defining LBRL and BLE for: a – SUV; b – compact vehicle with a wedge-shaped body

2.3. Selection of parameters to define the kinematics of the dummy

In order to develop the kinematic criterion it was necessary to choose such functions defining the geometric properties of dummy motion that would determine, directly or after appropriate mathematical transformations, the kinematics of the pedestrian dummy after a collision with a vehicle.

The main problem was to establish guidelines that would clearly indicate the location, method and object of measurements. The measurement spectrum of numerical methods is significant as it can be used to determine, in a reproducible manner, the displacements and their derivatives at each time step. The MADYMO application code includes a series of parameters for the dummy database, which determine the possibility of body injury, such as the HIC criterion and the distribution of forces over time for each kinematic joints (Anderson *et al.* 2007; Fernandes *et al.* 2018; TNO 2012). The aim of the work, however, was to determine such parameters that could, in the future, be defined not only for a virtual pedestrian dummy, but also – after appropriate adjustments – for a physical pedestrian dummy. Based on preliminary tests of the vehicle to dummy collision, the following variables were selected, which can be used to determine the geometric properties of the post-impact dummy motion:

- the kinetic energy of dummy linear motion E_{k_p} and the kinetic energy of dummy curvilinear motion $E_{k\_k;}$
- momentum p and angular momentum L of the dummy;
- linear acceleration a and angular acceleration ε of the dummy's center of mass (GoG);
- linear velocity v and angular velocity ω of the GoG.

The decision to determine the linear velocity v and angular velocity ω of the GoG was made for the following reasons:

- in tests on real objects it would be technically difficult to determine the ratio of kinetic energy of linear motion to kinetic energy of curvilinear motion of the dummy;
- in order to measure the momentum and angular momentum, the dummy would have to be considered as a rigid body (unacceptable simplification) or the linear and rotational velocity would have to be calculated separately for each segment (a time-consuming process);
- functions of linear and angular acceleration for the issue under investigation are highly changeable in the time domain and, without the use of suitable filtering, are not smooth functions;
- mathematically, it is relatively simple to determine the global extreme for the function of linear and angular velocity in time due to the smooth course of the two functions for the presented phenomenon;
- the analysis of the functions $v(t)$ and $\omega(t)$ is simpler if data filters are not used.

2.4. Parameter *k* for validating pedestrian kinematics

In order to develop the k parameter, based on an analysis of the linear velocity v and angular velocity ω of the MADYMO GoG as a function of time, the following assumptions were made:

The pedestrian's center of mass is positioned in the center of symmetry of the rigid ellipsoid called *pelvis_bod* (Figure 3) – this assumption is consistent with the conclusions of Simms and Woods (2009) and with the TNO (2012) guidelines:

- the choice of the coordinate system:
  - the angular velocity ω is measured in relation to the x axis of the local coordinate system located in the *pelvis_bod* ellipsoid; the orientation of axes in the local coordinate system is consistent with the global coordinate system during the entire simulation;
  - the linear velocity v is measured in relation to the Y-axis of the global, fixed coordinate system;
- the value of angular velocity ω is defined as positive when its orientation is aligned with the X-axis and the vehicle is moving in the direction of Y-axis;
- the linear velocity v is defined positive when the pedestrian's center of mass is moving in the direction of Y-axis;
- the time range t was limited to 0.2 s – within this time range the kinematics of the pedestrian is already clearly established for the adopted configuration of ellipsoids that define the LBRL and BLE of the vehicle;
- the sampling rate of values v and ω was set at 10000 Hz;
- the unknown values of functions $v(t)$ and $\omega(t)$ are *global extremes* of these functions in the time domain $0 < t \leq 0.2$ s;
- then, based on the abovementioned assumptions, the k parameter is calculated using the formula (1):

$$k = \begin{cases} \dfrac{\min(\omega(t))}{\max(v(t))}, & \text{for } \left|\min(\omega(t))\right| \geq \left|\max(\omega(t))\right|; \\ \dfrac{\max(\omega(t))}{\max(v(t))}, & \text{for } \left|\min(\omega(t))\right| < \left|\max(\omega(t))\right|. \end{cases} \quad (1)$$

An example of an impact simulation for a male 50-percentile dummy with the configuration of ellipsoids $LBRL$ = 0.47 m and BLE = 0.92 m and D = 0.45 m was depicted in Figure 5. In this impact configuration, the pedestrian is wrapped around the vehicle model. Figure 5 shows also the graphs of kinematic functions of linear and curvilinear motion of the GoG for the abovementioned impact configuration.

Further analysis uses the functions of linear velocity $v(t)$ and angular velocity $\omega(t)$, for which the global extremes were determined, in particular the global maxima in the range $0 < t \leq 0.2$ s. Note that function $\omega(t)$ takes positive values throughout its domain because the pedestrian's center of mass rotates towards the vehicle for the duration of impact. The formula includes a case where: $\left|\min(\omega(t))\right| < \left|\max(\omega(t))\right|$.

For the registered functions, the value of k parameter was determined using the formula (2):

$$k = \frac{\max(\omega(t))}{\max(v(t))} = \frac{21.72 \text{ rad/s}}{10.97 \text{ m/s}} = 1.98 \text{ rad/m}. \quad (2)$$

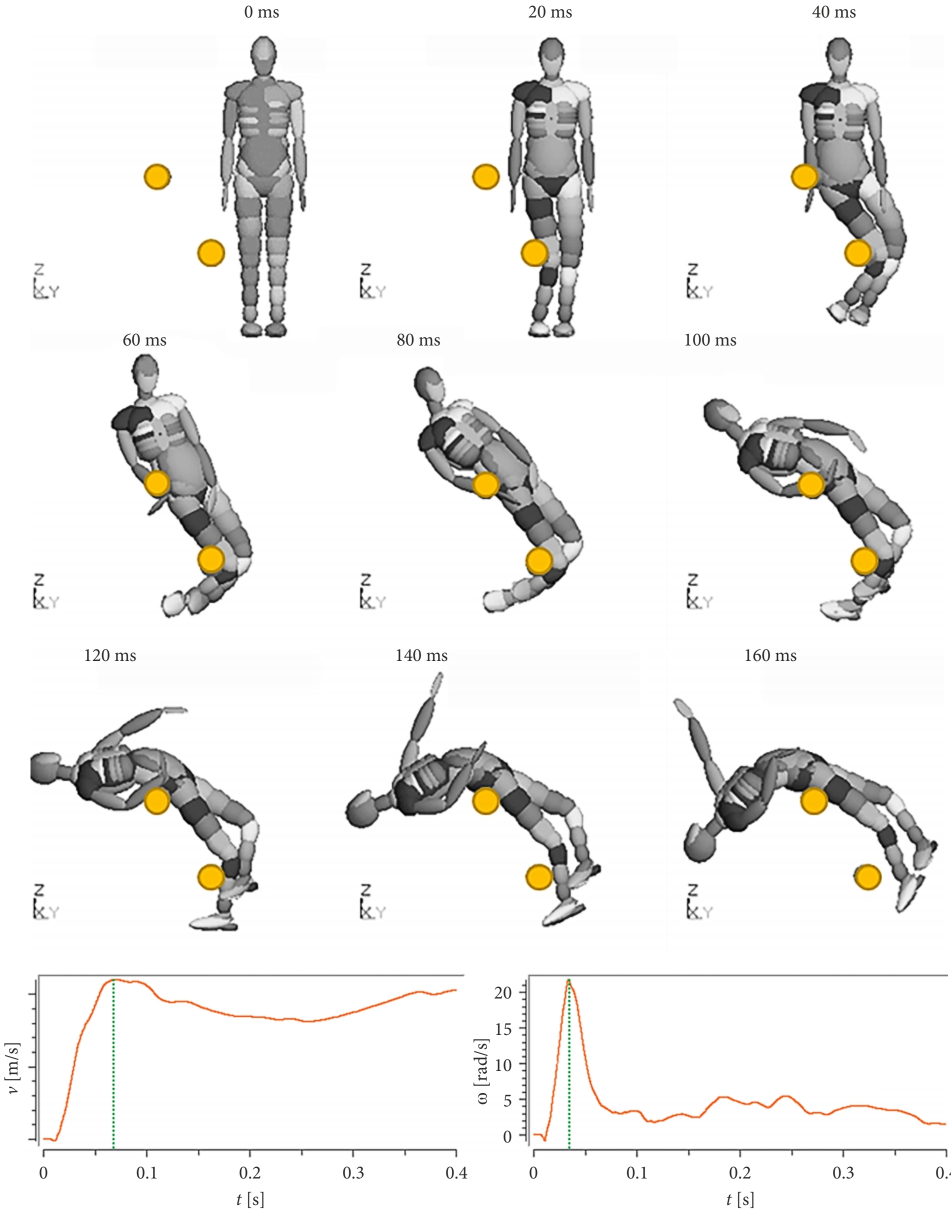

Figure 5. Example of a collision simulation for a male 50-percentile dummy model and graphs of functions $v(t)$ and $\omega(t)$ of dummy's center of mass (CoG)

3. Results

A total of 80 simulations were performed of the impact of the ellipsoid system, which defines the LBRL and BLE, into a 50-percentile male dummy and a 5-percentile female dummy. The result of these simulations is the distribution of values of the k parameter for the registered post-impact dummy kinematics. Figure 6 shows the correlation of parameter k on the pedestrian dummy kinematics. The dependence of k on the geometric characteristics of post-impact dummy motion is more noticeable when the values of parameter k are presented in descending order.

What is characteristic for the performed simulations is that when:

- $2.24 \geq k \geq 1.69$ rad/m – the pedestrian is wrapped over the vehicle model;
- $1.55 \geq k \geq 0.74$ rad/m – the pedestrian is projected forward;
- $-0.32 \geq k \geq -2.30$ rad/m – the pedestrian is dragged underneath the vehicle.

The above relationship leads to the conclusion that the k parameter can be used to validate the kinematics of the pedestrian after a collision with a motor vehicle. Finally, after analysing the trends in results, the following values of parameter k were adopted to validate the post-impact kinematics of the pedestrian (3):

$k \geq 1.7$ rad/m – wrap projection;
$0 \leq k < 1.7$ rad/m – forward projection;
$k < 0$ rad/m – dragging underneath the vehicle. (3)

Thus, the kinematic criterion was defined as follows: a motor vehicle provides tolerable post-impact kinematics for the pedestrian when: $k \geq 1.7$ rad/m.

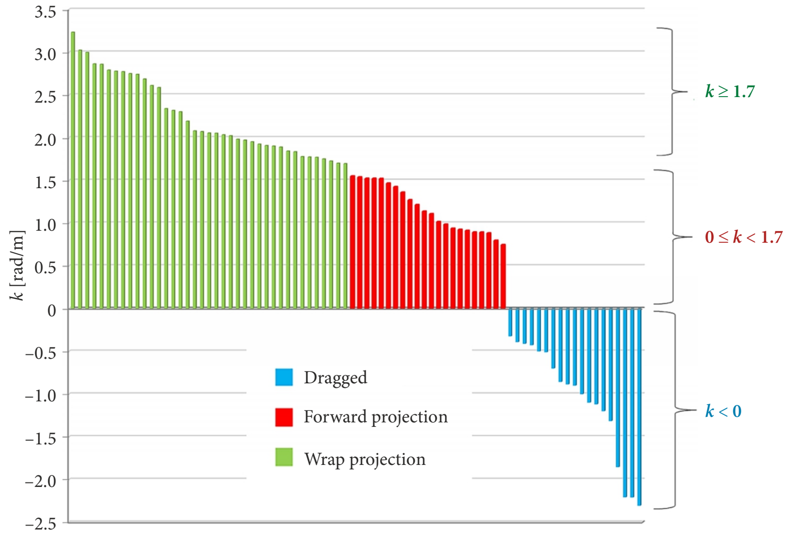

Figure 6. Sorted values of the k parameter with respect to post-impact pedestrian kinematics

4. Discussion

The current vehicle testing methods do not fully assess the actual risks posed to pedestrians by SUVs. With the growing popularity of SUVs, assessment of such vehicles only on the basis of tests using impactors may be not reliable, as demonstrated in the publications by Matsui (2004), Matsui *et al.* (2005) and Ptak *et al.* (2012).

By finding the correlation between the kinematics of the dummy under test and the value of parameter k, it was possible to develop a method of assessing the influence of structural components of the vehicle's front end on pedestrian safety during a collision. The developed method combines the kinematic criterion k, and the biomechanical criterion, i.e. the testing of vehicles using impactors. The new method can be applied both in numerical tests, which were the basis of the method itself, as well as in tests using a physical dummy. It should be mentioned, however, that the application of the method on a real object requires the parameter k to be accordingly adjusted.

A following procedure was proposed for testing vehicles without the Frontal Protection System (FPS). The method consists of 4 main stages:

– ***Stage 1: measurement of the vehicle and choice of the dummy for testing:***

This stage involves measurements of the LBRL and the BLE in accordance with the guidelines in Figure 2. The measurement is carried out on a real object or a geometric model of the vehicle in any CAD/CAE application.

In the next step, a dummy is chosen for tests. 2 types of dummies are available:
- 50-percentile male – for standard tests, including type-approval;
- 5-percentile female – for more demanding vehicle tests designed to also ensure the safety of shorter pedestrians.

– ***Stage 2: categorization of the vehicle:***

In this stage, the following calculations are made based on the geometric relationships between the test vehicle and the dummy:
- the ratio of the height of the BLE to the height of the dummy H:

$$\frac{BLE}{H}; \tag{5}$$

- the ratio of the height of the BLE to the height of the CoG:

$$\frac{BLE}{CoG}. \tag{6}$$

Based on formulae (5) and (6) and the vehicle's LBRL value, the following conditions are validated:

A: $\frac{BLE}{H} \geq 0.75;$

B: $\frac{BLE}{CoG} \geq 1.00;$

C: $LBRL > 425\,\text{mm}.$

There are 3 possible outcomes of the decision-making process:

1) *fulfilment of condition A* – the vehicle does not satisfy the kinematic criterion; the requirements of this stage can be met if a FPS is used.

Explanation: the BLE height is above 75% of dummy height – the vehicle strikes the pedestrian at chest level and therefore adequate post-impact kinematics of the pedestrian cannot be ensured;

2) *the condition* $A \wedge B \wedge C$ *is not fulfilled* – validation of the kinematic criterion for the tested vehicle in not necessary; the process proceeds directly to Stage 4.

Explanation: the geometric features of the vehicle provide adequate post-impact kinematics of the pedestrian;

3) *condition A is not fulfilled, whereas condition* $B \vee C$ *is fulfilled* – the vehicle model must be tested with a dummy and the value of parameter *k* must be validated in Stage 3.

Explanation: the front-end geometry of the vehicle may endanger pedestrians during accidents.

– ***Stage 3: validation of the kinematic criterion***

This stage involves the final validation of the kinematic criterion. Based on the results of numerical simulations and physical tests (after appropriate adjustment of parameter *k*):

1) $k \geq 1.7$ rad/m – the pedestrian is wrapped;
2) $0 \leq k < 1.7$ rad/m – the pedestrian is projected forward;
3) $k < 0$ rad/m – the pedestrian is dragged underneath the vehicle.

The vehicle meets the kinematic criterion (or shall be equipment with pedestrian FPS) and proceeds to Stage 4 if the value of $k \geq 1.7$ rad/m.

– ***Stage 4: validation of the biomechanical criterion according to the Regulation (EC) No 78/2009***

Validation involves tests of the vehicle front using impactors in accordance with current standards and *Regulation (EC) No 78/2009* (EC 2009b; Ptak *et al.* 2017a). It should be noted that only those vehicles reach Stage 4, which have previously been categorized as safe in terms of the kinematic criterion (Stage 3) or their geometry has been arbitrarily categorized as safe (Stage 2, unfulfilled condition $A \wedge B \wedge C$). If the vehicle meets the requirements of Stage 4, it is categorized as safe in accordance with the kinematic and biomechanical criteria.

Conclusions

This investigation was inspired by the problem of safety testing of SUVs with respect to pedestrian protection. Namely, the discrepancy between the values of bending angle in the knee joint during tests on sport-utility vehicles using a legform impactor and pedestrian dummy – significant differences can be observed in the knee bending angle of the dummy and the impactor (Ptak *et al.* 2012). Moreover, the results of standard type-approval tests with the legform impactor can lead to a positive evaluation of the safety of vehicles, which in fact could cause serious injury to pedestrians during accidents. In addition, tests performed in accordance with *Regulation (EC) No 78/2009* do not represent the full kinematics of the collision, which are very significant in terms of pedestrian injuries. Therefore, a new method was developed to assess the influence of structural components of vehicles on pedestrian safety.

The study, which led to the development of a new method, also included tests focusing on the validation of post-impact pedestrian kinematics. A parametric model of the vehicle was generated, based on the appropriate position configuration of ellipsoids. The use of a series of configurations of ellipsoids allowed the front-end geometry to be represented for typical vehicles. A 50-percentile male dummy and a 5-percentile female dummy were used in the tests. The use of a female dummy expanded the spectrum of research by issues related to collisions of vehicles with shorter pedestrians.

By analysing the linear velocity *v* and angular velocity ω of the ellipsoid located in the center of mass of a given dummy, the kinematics of the pedestrian dummy were properly defined, which contributed to the development of a new *k* parameter. Numerical simulations of the impact of a system of ellipsoids into dummies indicated that parameter *k* depends on the post-impact kinematics of the pedestrian. It was proved that for a given value of parameter *k* particular post-impact kinematics of the pedestrian can be observed, i.e.: wrap projection, forward projection or dragging of the pedestrian underneath the vehicle. Therefore, it is possible to pre-evaluate the safety of a motor vehicle with regard to pedestrian protection. The performed tests have shown that a motor vehicle provides satisfactory kinematics to the pedestrian after impact when $k \geq 1.7$ rad/m. This relationship was called the kinematic criterion. Thus, the main goal of this paper has been fulfilled. The future research may encompass the development of the dependence of parameter *k* in the function of variable impact velocities and pedestrian stance during an accident.

It is worth noting that the method of testing vehicle safety permits the use of a FPS also in a vehicle, which does not meet the requirements of Stage 2 or 3. According to the developed method, in the case of a negative result of the initial validation of the vehicle, by using the FPS it is still possible for the vehicle to obtain another positive evaluation, without the need to introduce expensive changes to the vehicle's front-end structure.

Acknowledgements

The publication was developed as part of project 2011/03/N/ST8/05927 supported by the National Science Centre, Poland.

References

Anderson, R. W. G.; McLean, A. J.; Farmer, M. J. B.; Lee, B. H.; Brooks, C. G. 1997. Vehicle travel speeds and the incidence of fatal pedestrian crashes, *Accident Analysis* & *Prevention* 29(5): 667–674. https://doi.org/10.1016/S0001-4575(97)00036-5

Anderson, R. W. G.; Streeter, L. D.; Ponte, G.; McLean, J. 2007. Pedestrian reconstruction using multibody MADYMO simulation and the Polar-II Dummy: a comparison of head kinematics. Paper No 07-0273, in *20th International Technical Conference on the Enhanced Safety of Vehicles (ESV)*, 18–21 June 2007, Lyon, France, 1–15.

Asaithambi, G.; Kuttan, M. O.; Chandra, S. 2016. Pedestrian road crossing behavior under mixed traffic conditions: a comparative study of an intersection before and after implementing control measures, *Transportation in Developing Economies: a Journal of the Transportation Research Group of India* 2:14. https://doi.org/10.1007/s40890-016-0018-5

Cesari, D.; Cavallero, C.; Farisse, J.; Bonnoit, J. 1985. Effects of crash conditions on pedestrian leg kinematics and injuries based on cadaver and dummy tests, in *29th Annual Conference of the American Association for Automotive Medicine*, 7–10 October 1985, Washington, DC, US, 275–285.

Chybowski, L.; Idziaszczyk, D.; Wiśnicki, B. 2014. A comparative components importance analysis of a complex technical system with the use of different importance measures, *Systems Supporting Production Engineering: Review of Problems and Solutions* 1(7): 22–33.

Crocetta, G.; Piantini, S.; Pierini, M.; Simms, C. 2015. The influence of vehicle front-end design on pedestrian ground impact, *Accident Analysis & Prevention* 79: 56–69. https://doi.org/10.1016/j.aap.2015.03.009

DYNAmore. 2018. *Human Model*. DYNAmore GmbH. Available from Internet: https://www.dynamore.de/en/products/models/human

EC. 2009a. *Commission Regulation (EC) No 631/2009 of 22 July 2009 Laying Down Detailed Rules for the Implementation of Annex I to Regulation (EC) No 78/2009 of the European Parliament and of the Council on the Type-Approval of Motor Vehicles with Regard to the Protection of Pedestrians and other Vulnerable Road Users, Amending Directive 2007/46/EC and Repealing Directives 2003/102/EC and 2005/66/EC*. 60 p. Available from Internet: http://data.europa.eu/eli/reg/2009/631/oj

EC. 2009b. *Regulation (EC) No 78/2009 of the European Parliament and of the Council of 14 January 2009 on the Type-Approval of Motor Vehicles with Regard to the Protection of Pedestrians and Other Vulnerable Road Users, Amending Directive 2007/46/EC and Repealing Directives 2003/102/EC and 2005/66/EC*. 31 p. Available from Internet: http://data.europa.eu/eli/reg/2009/78/oj

EC. 2015. *Road Safety in the European Union: Trends, Statistics and Main Challenges*. European Commission. 24 p. https://doi.org/10.2832/404614

Fernandes, F. A. O.; Pascoal, R. J. S.; De Sousa, R. J. A. 2014. Modelling impact response of agglomerated cork, *Materials & Design* 58: 499–507. https://doi.org/10.1016/j.matdes.2014.02.011

Fernandes, F. A. O.; Tchepel, D.; De Sousa, R. J. A.; Ptak, M. 2018. Development and validation of a new finite element human head model: yet another head model (YEAHM), *Engineering Computations* 35(1): 477–496. https://doi.org/10.1108/EC-09-2016-0321

Fricke, L. B. 1990. *Traffic Accident Reconstruction: Volume 2 of the Traffic Accident Investigation Manual*. Northwestern University Center for Public. 453 p.

Hamacher, M.; Eckstein, L.; Paas, R. 2012. Vehicle related influence of post-car impact pedestrian kinematics on secondary impact, in *2012 IRCOBI Conference Proceedings*, 12–14 September 2012, Dublin, Ireland, 717–729.

Henary, B. Y.; Crandall, J.; Bhalla, K.; Mock, C. N.; Roudsari, B. S. 2003. Child and adult pedestrian impact: the influence of vehicle type on injury severity, *Annual Proceedings, Association for the Advancement of Automotive Medicine* 47: 105–126.

IMPROVER. 2006. *Impact on Road Safety Due to the Increasing of Sports Utility and Multipurpose Vehicles*. Final Report TREN-04-ST-S07.37022. Impact Assessment of Road Safety Measures for Vehicles and Road Equipment (IMPROVER) Consortium. 169 p.

Ishikawa, H.; Kajzer, J.; Schroeder, G. 1993. Computer simulation of impact response of the human body in car-pedestrian accidents, *SAE Technical Paper* 933129: 1–14. https://doi.org/10.4271/933129

Jarrett, K. L.; Saul, R. A. 1998. Pedestrian injury-analysis of the PCDS field collision data, in *16th International Technical Conference on the Enhanced Safety of Vehicles (ESV)*, Windsor, Ontario, Canada, 31 May – 4 June 1998, 1204–1211.

Jurecki, R. S.; Stańczyk, T. L. 2014. Driver reaction time to lateral entering pedestrian in a simulated crash traffic situation, *Transportation Research Part F: Traffic Psychology and Behaviour* 27: 22–36. https://doi.org/10.1016/j.trf.2014.08.006

Kaczyński, P.; Bartczak, B. 2014. The influence of orientation of segmented die on clinch joints mechanical properties, *Journal of Machine Engineering* 14(3): 126–136.

Kadali, B. R.; Vedagiri, P. 2016. Proactive pedestrian safety evaluation at unprotected mid-block crosswalk locations under mixed traffic conditions, *Safety Science* 89: 94–105. https://doi.org/10.1016/j.ssci.2016.05.014

Kerrigan, J. R.; Arregui-Dalmases, C.; Foster, J., Crandall, J. R.; Rizzo, A. 2012. Pedestrian injury analysis: field data vs. laboratory experiments, in *2012 IRCOBI Conference Proceedings*, 12–14 September 2012, Dublin, Ireland, 672–689.

Kolla, E.; Kohút, P.; Kubjatko, T. 2014. Analysis of pedestrian body movement in pedestrian – MPV collision, in *IX Międzynarodowa Konferencja Naukowo-Techniczna – Automotive Safety 2014 – Problemy Bezpieczeństwa w Pojazdach Samochodowych*, 8–10 April 2014, Rajecké Teplice, Slovakia.

Kopczyński, A.; Ptak, M.; Harnatkiewicz, P. 2011. The influence of frontal protection system design on pedestrian passive safety, *Archives of Civil and Mechanical Engineering* 11(2): 345–364. https://doi.org/10.1016/S1644-9665(12)60148-4

Lefler, D. E.; Gabler, H. C. 2004. The fatality and injury risk of light truck impacts with pedestrians in the United States, *Accident Analysis & Prevention* 36(2): 295–304. https://doi.org/10.1016/S0001-4575(03)00007-1

Levulytė, L.; Baranyai, D.; Sokolovskij, E.; Török, Á. 2017. Pedestrians' role in road accidents, *International Journal for Traffic and Transport Engineering* 7(3): 328–341. https://doi.org/10.7708/ijtte.2017.7(3).04

Levulytė, L.; Baranyai, D.; Török, Á.; Sokolovskij, E. 2016. Bicycles' role in road accidents a review of literature, *Transport and Telecommunication Journal* 17(2): 122–127. https://doi.org/10.1515/ttj-2016-0011

Matsui, Y. 2004. Evaluation of pedestrian subsystem test method using legform and upper legform impactors for assessment of high-bumper vehicle aggressiveness, *Traffic Injury Prevention* 5(1): 76–86. https://doi.org/10.1080/15389580490430272

Matsui, Y.; Wittek, A.; Tanahashi, M. 2005. Pedestrian kinematics due to impacts by various passenger cars using full-scale dummy, *International Journal of Vehicle Safety* 1(1/2/3): 64–84. https://doi.org/10.1504/IJVS.2005.007538

Mizuno, Y. 2005. Summary of IHRA pedestrian safety WG activities (2005) – proposed test methods to evaluate pedestrian protection afforded by passenger cars, in *19th International Technical Conference on the Enhanced Safety of Vehicles (ESV)*, 6–9 June 2005, Washington, DC, US, 1–15.

Mizuno, Y. 2003. Summary of IHRA pedestrian safety WG activities (2003) – proposed test methods to evaluate pedestrian protection afforded by passenger cars, in *18th International Technical Conference on the Enhanced Safety of Vehicles (ESV)*, 19–22 May 2003, Nagoya, Japan, 1–17.

Nordfjærn, T.; Zavareh, M. F. 2016. Individualism, collectivism and pedestrian safety: a comparative study of young adults from Iran and Pakistan, *Safety Science* 87: 8–17. https://doi.org/10.1016/j.ssci.2016.03.005

Otte, D. 1999. Severity and mechanism of head impacts in car to pedestrian accidents, in *1999 IRCOBI Conference Proceedings*, 23–24 September 1999, Sitges, Spain, 329–341.

Pezowicz, C.; Głowacki, M. 2012. The mechanical properties of human ribs in young adult, *Acta of Bioengineering and Biomechanics* 14(2): 53–60. https://doi.org/10.5277/abb120207

Ptak, M.; Blicharski, P.; Rusiński, E.; Karliński, J. 2017a. Numerical simulations of composite frontal protection system according to EC 78/2009, in *Proceedings of the 13th International Scientific Conference: Computer Aided Engineering*, 423–429. https://doi.org/10.1007/978-3-319-50938-9_44

Ptak, M.; Kaczyński, P.; Fernandes, F.; De Sousa, R. A. 2017b. Computer simulations for head injuries verification after impact, in E. Rusiński, D. Pietrusiak (Eds.). *Proceedings of the 13th International Scientific Conference: Computer Aided Engineering*, 431–440. https://doi.org/10.1007/978-3-319-50938-9_45

Ptak, M.; Karliński, J. 2012. Pedestrian passive safety during the SUV impact: regulations vs. reality, in *2012 IRCOBI Conference Proceedings*, 12–14 September 2012, Dublin, Ireland, 103–113.

Ptak, M.; Konarzewski, K. 2015. Numerical technologies for vulnerable road user safety enhancement, *Advances in Intelligent Systems and Computing* 354: 355–364. https://doi.org/10.1007/978-3-319-16528-8_33

Ptak, M.; Rusiński, E.; Karliński, J.; Dragan, S. 2012. Evaluation of kinematics of SUV to pedestrian impact – lower leg impactor and dummy approach, *Archives of Civil and Mechanical Engineering* 12(1): 68–73. https://doi.org/10.1016/j.acme.2012.03.016

Ratajczak, M.; Sąsiadek, M.; Będziński, R. 2016. An analysis of the effect of impact loading on the destruction of vascular structures in the brain, *Acta of Bioengineering and Biomechanics* 18(3): 21–31. https://doi.org/10.5277/ABB-00552-2016-02

Rosén, E.; Stigson, H.; Sander, U. 2011. Literature review of pedestrian fatality risk as a function of car impact speed, *Accident Analysis & Prevention* 43(1): 25–33. https://doi.org/10.1016/j.aap.2010.04.003

Roudsari, B. S.; Mock, C. N.; Kaufman, R.; Grossman, D.; Henary, B. Y.; Crandall, J. 2004. Pedestrian crashes: higher injury severity and mortality rate for light truck vehicles compared with passenger vehicles, *Injury Prevention* 10(3): 154–158. https://doi.org/10.1136/ip.2003.003814

Simms, C. K.; Wood, D. P. 2009. *Pedestrian and Cyclist Impact: a Biomechanical Perspective*. 230 p. https://doi.org/10.1007/978-90-481-2743-6

Simms, C. K.; Wood, D. P. 2006. Pedestrian risk from cars and sport utility vehicles – a comparative analytical study, *Proceedings of the Institution of Mechanical Engineers, Part D: Journal of Automobile Engineering* 220(8): 1085–1100. https://doi.org/10.1243/09544070JAUTO319

Simms, C. K.; Wood, D.; Fredriksson, R. 2015. Pedestrian injury biomechanics and protection, in N. Yoganandan, A. M. NahumJohn, W. Melvin (Eds.). *Accidental Injury*, 721–753. https://doi.org/10.1007/978-1-4939-1732-7_24

Sokolovskij, E.; Prentkovskis, O. 2013. Investigating traffic accidents: the interaction between a motor vehicle and a pedestrian, *Transport* 28(3): 302–312. https://doi.org/10.3846/16484142.2013.831771

Stevenson, T. J. 2006. *Simulation of Vehicle-Pedestrian Interaction*. PhD Thesis. University of Canterbury, New Zealand. 342 p. Available from Internet: https://ir.canterbury.ac.nz/handle/10092/1180

Teresiński, G. 2005. *Biomechanika potrąceń pieszego*. Wydawnictwo. Akademii Medycznej w Lublinie. 1–87. (in Polish).

TNO. 2012. *MADYMO: Human Body Models Manual*. Release 7.4.1. The Netherlands Organization for Applied Scientific Research (TNO). 122 p.

Yang, J. 2005. Review of injury biomechanics in car-pedestrian collisions, *International Journal of Vehicle Safety* 1(1/2/3): 100–117. https://doi.org/10.1504/IJVS.2005.007540

Yasuki, T.; Yamamae, Y. 2010. Validation of kinematics and lower extremity injuries estimated by total human model for safety in SUV to pedestrian impact test, *Journal of Biomechanical Science and Engineering* 5(4): 340–356. https://doi.org/10.1299/jbse.5.340

Zalewski, R.; Szmidt, T. 2014. Application of special granular structures for semi-active damping of lateral beam vibrations, *Engineering Structures* 65: 13–20. https://doi.org/10.1016/j.engstruct.2014.01.035

Zhang, G.; Cao, L.; Hu, J.; Yang, K. H. 2008. A field data analysis of risk factors affecting the injury risks in vehicle-to-pedestrian crashes, *Annals of Advances in Automotive Medicine* 52: 199–214.

Żółkiewski, S. 2011. Testing composite materials connected in bolt joints, *Journal of Vibroengineering* 13(4): 817–822.